

# The wildlands connectivity dilemma: a graph-theory computational approach

Simon Jean\*<sup>1</sup> and Lauriane Mouysset<sup>1</sup>

<sup>1</sup>CIREC, Ecole des Ponts, AgroParisTech, EHESS, CIRAD, CNRS, Université Paris-Saclay, Nogent-sur-Marne, France

January 25, 2024

## Abstract

**Background:** Fuel treatment operations help to mitigate the spread and severity of wildfires in numerous ecosystems. As they aim at fragmenting the fire landscape, they also fragment wildlife habitat. This poses a dilemma for land managers, in the form of a trade-off between lowering wildfire patch connectivity and maintaining wildlife habitat connectivity. Previous studies have investigated the spatial allocation of fuel treatments over time, mostly without specific care devoted to biodiversity, in a variety of case studies. However, they lack generality and an interpretative framework. We use dynamic programming and graph theory on every possible theoretical landscape configuration to gain a general understanding of the allocation of treatments over space and time and the corresponding landscape properties with various habitat connectivity targets.

**Results:** Our results show that all initial landscapes converge to steady-state landscape cycles. Moreover, we show that there exist optimal trajectories that significantly reduce wildfire risk while safeguarding habitat connectivity. As the policy budget increases, more risk reduction is achieved, albeit with a decreasing marginal efficiency, and more steady-state cycles emerge. As habitat targets increase, increasing the budget is of no effect, and risk increases, while the number of steady-state cycles decreases. Landscapes are less risky, more fragmented, and diverse when the budget is large and biodiversity targets are low, while they are more compact and less diverse when the opposite is true. Treatment allocation follows graph centrality measures, and central cells are treated first. When the budget increases, fewer central cells (i.e. edge patches) are treated as well. When biodiversity targets increase, central cells are no longer treated as they decrease habitat connectivity. Treatment is reshuffled to the edges of the landscape.

**Conclusion:** Computational experiments generalize existing results. Using graph theory, general insights can be gained, and help managers faced with multiple objectives in forested landscapes. From a policy perspective, in the face of climate change, increasing treatment budgets should be a priority to avoid increasing damages. A key guideline is treating a variety of seral stages to create landscape diversity, mitigate risk and guarantee the connectivity of wildlife habitat.

**Keywords :** Fuel treatment, connectivity, wildfire risk, wildlife habitat, spatial optimization, graph theory

## 1 Introduction

Hazardous and intense wildfires threaten forest resilience and can cause ecosystem shifts (Coop et al. 2020). They also cause dramatic impacts on biodiversity across taxa (Wintle et al. 2020). Moreover, intense wildfires cause human damages, in the form of direct asset losses: in 2018, wildfires in California have caused \$ 27 billion (Wang et al. 2021). Indirect costs are also of concern, especially related to wildfire smoke (increase in PM 2.5 concentrations have important health impacts (Burke et al. 2023, Heft-Neal et al. 2023), recreation values are affected in the US, amounting to \$USD 2.3 billion (Gellman et al. 2023)). Eventually, large wildfires are of importance in the face

---

\*Corresponding author : jean@centre-cired.fr

8 of climate change releasing a lot of greenhouse gas and reducing the atmospheric carbon sinks (Zheng et al. 2023,  
9 Sweeney et al. 2023). Global warming affects water supply and fuel moisture (Jolly et al. 2015, Abatzoglou and  
10 Williams 2016, Ruffault et al. 2018), and is projected to increase the frequency, severity, and magnitude of wildfires  
11 (Wasserman and Mueller 2023). Recent wildfire events in California (since 2018), in Australia (2019-2020), and in  
12 Europe (France, Portugal, Greece in 2022) have epitomized these trends.

13 In numerous regions, such as conifer forests in California (Vaillant et al. 2009, Kalies and Yocom Kent 2016,  
14 Low et al. 2023), eucalypt forests in South Western Australia (Burrows and McCaw 2013, Boer et al. 2009, Florec  
15 et al. 2020), southern Europe (Fernandes et al. 2013), evidence shows that fuel treatments (e.g. prescribed burns,  
16 mechanical thinning and managed wildfires), can mitigate wildfire intensity and spread. Land management agencies  
17 have historically implemented these policies in Australia (Burrows and McCaw 2013), Europe, and the United States  
18 (and are projected to ramp up, for example under the Infrastructure Investment and Jobs Act of 2021 in the US).  
19 Understanding the spatial allocation of treatments, as climate change impacts negatively both costs and feasibility,  
20 is a major driver of policy success (Williams et al. 2017, Florec et al. 2020).

21 By changing the structure of the landscape, fuel management operations also affect the structure of biodiversity  
22 habitat, notably, its structural connectivity (Taylor et al. 1993). Maintaining habitat connectivity, through wildlife  
23 corridors, landscape links, and ecoducts (Turner 2005, Turner and Gardner 2015), is instrumental in mitigating the  
24 biodiversity crisis. Species richness and diversity are intimately linked to landscape connectivity (Olds et al. 2012,  
25 Tian et al. 2017, Velázquez et al. 2019) and are necessary to maintain ecosystems in the future. The impact of fuel  
26 treatments on biodiversity remains a debated topic. Evidence suggests that maintaining a variety of vegetation  
27 types and ages on a patchy landscape maintains a 'fire mosaic' (Sitters et al. 2015) (e.g. landscape level variations in  
28 habitat types that provide habitat to an ecological community) or that fuel treatment can be beneficial to wildlife  
29 (Saab et al. 2022, Loeb and Blakey 2021) and even restore local populations (Templeton et al. 2011). On the  
30 other hand, treating at too high a frequency may be detrimental to biodiversity (Bradshaw et al. 2018). Overall,  
31 implementing fuel treatment challenges the connectivity of wildlife habitat. In this context, understanding the  
32 trade-offs between risk reduction and biodiversity conservation, as well as the spatial patterns of operations that  
33 could reconcile the two objectives is key. In this study, we investigate the spatial allocation of fuel treatments to  
34 optimally reduce wildfire risks while maintaining biodiversity habitat.

35 A substantial literature has applied optimization techniques to tackle the spatial allocation of fuel treatments.  
36 Analytical (Finney 2001), simulation-based (Finney 2007, Rytwinski and Crowe 2010) or mixed-integer program-  
37 ming techniques (Wei et al. 2008) have solved the allocation of treatments in a static framework. Given the dynamic  
38 nature of fuel growth, studies based on mixed-integer dynamic programming (Wei et al. 2008, Minas et al. 2014,  
39 Rachmawati et al. 2015; 2016) have studied the temporal and spatial allocation of fuel treatments on real and  
40 simulated landscapes. While they solve the spatial treatment allocation problem in forests, these articles fail to  
41 acknowledge the multiple uses and objectives land planners have to consider, such as habitat conservation. Several

42 articles have devoted their attention to the spatial allocation of treatments while conserving habitat, and inves-  
43 tigated the trade-offs between risk reduction and biodiversity conservation, using spatial heuristics (Calkin et al.  
44 2005, Lehmkuhl et al. 2007) and linear programming (Williams et al. 2017, Rachmawati et al. 2018). Most of the  
45 existing literature focuses on case studies and lacks a general interpretative framework to generalize its results.  
46 Graph theory offers a toolbox suited to analyze the properties of connected patches of land with varying charac-  
47 teristics, and has extensively been applied in landscape ecology (Urban and Keitt 2001, Minor and Urban 2008,  
48 Rayfield et al. 2016). Recent research focusing on the allocation of fuel treatments has leveraged tools from graph  
49 theory (Matsypura et al. 2018, Pais et al. 2021a). Reconciling habitat and wildfire risk mitigation using graph  
50 theory is a recent research endeavor (Rachmawati et al. 2018, Yemshanov et al. 2022) and has focused on specific  
51 case studies.

52 In this article, we leverage graph theory on an exhaustive set of theoretical landscapes to study the general  
53 patterns of treatment allocation emerging from a multi-objective, dynamic, and integer landscape management  
54 problem, governed by connectivity. We analyze all the landscape configurations resulting from a 20-period planning  
55 horizon, for regular grid landscapes, in a graph theoretical perspective. In doing so, we examine the fuel treatment  
56 patterns resulting from all the range of habitat connectivity, in order to characterize long-term landscape properties.  
57 We characterize the landscapes using a range of ecological indicators and find general mechanisms and guiding  
58 principles applicable to a broad class of settings, to guide decision-makers and foster new efficient multi-objective  
59 graph theory algorithms.

60 Our contributions are several. First, we provide a spatial framework to understand the trade-offs between  
61 wildfire risk reduction and biodiversity conservation. Using graph theory, we derive general principles regarding  
62 the spatial characteristics of landscapes and treatments from an exhaustive set of theoretical landscapes to guide  
63 policymakers as well as future research in heuristics to reconcile conflicting land-based phenomena. Eventually,  
64 we characterize the risk and biodiversity profiles consistent with a changing climate, where windows of opportunity  
65 are shorter and costs of treatment larger, and the associated spatialized treatments.

## 66 2 Methods

### 67 2.1 Theoretical model

68 We consider theoretical landscapes represented by a regular grid of  $n \times n$  cells with a forest seral stage succession  
69 module. We use a stylized representation of the link between vegetation age, habitat, and wildfire risk. We denote  
70 by  $A_t$  the set of equal, standardized area cells in the theoretical landscape of dimension  $n \times n$  (hereafter referred  
71 to as being of size=  $n$ ) in period  $t$ . Each cell  $a_i$  at time  $t$  is characterized by a seral stage: absent, young, or old.  
72 At each time step, it changes stage until it is in the 'old' stage, where it remains. Upon treatment, a cell's seral  
73 stage is set to 'absent' (see equation A.1 in appendix A).

74 A cell offers wildlife habitat once it is 'mature' (eg seral stage is at least 'young'), i.e, when the time elapsed since  
75 the last burn reaches the maturity threshold (eq. A.2). We assume that habitat quality is uniformly distributed  
76 among habitat patches and that neighboring cells are reachable, conditional on being 'mature'. After the wildlife  
77 habitat maturity threshold, a cell can turn at critical risk of wildfire during a 'normal' hot season. We assume an  
78 Olsen-type model of flammability (Olson 1963, McCarthy et al. 2001), where age is the main predictor. Therefore,  
79 after the 'high fuel load' threshold is crossed, the cell is regarded as 'high risk' from then on, until treatment  
80 suppresses this risk (eq. A.3).

81 We define cells to be connected if (i) they are within an 8-cell neighborhood and (ii) share the same status.  
82 Regarding biodiversity, we focus on general characteristics related to landscape structural connectivity rather than  
83 functional connectivity, as we are agnostic about effective species (Fahrig et al. 2011). We assume that species are  
84 able to disperse from one patch to another, and that habitat quality is uniformly distributed conditional on habitat  
85 being available. We consider the wildfire risk through the lens of potential spread, which is only driven by fuel.  
86 Consistent with the literature (see Peterson et al. (2009), Pais et al. (2021b), Gonzalez-Olabarria et al. (2023)), a  
87 wildfire can spread in any direction, conditional on neighbor cells with high risk. However, if surrounding cells do  
88 not display high risk, fire does not spread.

89 We use a network structure to apprehend the landscapes. We transform  $A_t$  the set of cells constituting the  
90 landscape into graphs  $G_t$  whose vertices  $V_t$  (or nodes) are the cells in the landscape, and edges  $E_t$  represent the  
91 connections between cells. We partition the landscape in two graphs,  $G_{B_t}$  and  $G_{F_t}$ , each describing the network  
92 of mature habitat and risky patches (see fig. 1 for a representation). Landscape ecology has long used numerous,  
93 theoretically grounded indicators to analyze landscapes (Urban and Keitt 2001, Minor and Urban 2008). We use  
94 a global connectivity indicator that satisfies Pascual-Hortal and Saura (2006) criteria, grounded in graph theory,  
95 that offer a reformulation of Rachmawati et al. (2016) (see Appendix A.3).

96 We define the global connectivity index of habitat and risky patches in landscape  $A(t)$  as:

$$H_i(A(t)) = \text{card}(V_{i_t}) + 2 \times \text{card}(E_{i_t}) \text{ with } i \in \{B, F\} \quad (2.1)$$

97 This indicator considers that a habitat patch is connected to itself (i.e, within a habitat patch, there is no  
98 barrier) and whether it is connected to other patches. It implies lower connectivity when the distance between  
99 patches increases, attains its maximum value when a single habitat patch covers the whole landscape, indicates  
100 lower connectivity as the habitat is progressively more fragmented, considers negative the loss of a connected or  
101 isolated patch, and detects as more important the loss of bigger patches, of key and less important steppingstone  
102 patches.

103 To manage the expected damages resulting from wildfires, the land planner can decide to undertake specific  
104 treatments, in the form of a combination of controlled burns and/or mechanical thinnings. Upon treatment, we

105 assume that vegetation age in the cell is reset to 'absent': the wildfire risk vanishes, but so does the habitat and  
106 its connection to surrounding cells. Given the tension between maintaining habitat and reducing wildfire risk,  
107 the land planner aims to minimize a deterministic measure of connectivity of the high fuel loads in the landscape  
108 while maintaining a given level of biodiversity habitat connectivity under a budget constraint, over a planning  
109 horizon of length  $T$ . For the sake of the analysis, we focus on two layers of complexity over time and space: risk  
110 connectivity and biodiversity habitat. We do not consider heterogeneity in the economic costs or benefits (i.e.,  
111 homogeneous treatment costs and no patch-specific asset to protect). The framework is however amenable to such  
112 a prioritization. We also assume that the budget cannot be banked, and has to be utilized in each period, consistent  
113 with operational rules. Moreover, as the budget is constrained in each period, the measure of risk is bounded and  
114 the planning horizon is finite, we rule out discounting and assume each generation matters as much to the social  
115 planner.

116 The optimization problem is :

$$\min_x \left[ \sum_{t=1}^T H_F(A(t)) \right] \quad (2.2)$$

Such that:

$$A_i(t+1) = \min((A_i(t) + 1)(1 - x_i(t)), 2), \quad t = 1, \dots, T, \quad \forall i \in C \quad (2.3)$$

$$H_B(A(t)) \geq Biod, \quad t = 1, \dots, T \quad (2.4)$$

$$\sum_i x_i(t) \leq Budget, \quad t = 1, \dots, T \quad (2.5)$$

$$A(0) \text{ given} \quad (2.6)$$

$$x(t) \in \{0, 1\}^{n^2} \quad (2.7)$$

117 We abstract from decision-making in a risky environment, as it has been extensively described in economics  
118 and decision theory (Mouysset et al. 2013). Moreover, we mimic the role of risk aversion by varying the level of  
119 habitat connectivity constraint the decision maker chooses. We solve the dynamic, integer program of the landscape  
120 manager using dynamic programming. Dynamic programming provides a temporal decomposition of the initial  
121 problem defined over  $T$  periods, into  $T$  simpler problems, as it relies on the 'optimality principle'<sup>1</sup>. Second, it  
122 provides feedback controls which are know to be more adaptive especially if shocks occur or uncertainties affect the  
123 states or the dynamics of the system . The outputs of the method are both the optimal policies  $x_j^*(t, A)$ , i.e, the  
124 sequence of optimal controlled burns, and the optimal states  $A_j^*(t, A_0)$  resulting from the optimal policies and the  
125 initial conditions

---

<sup>1</sup>"An optimal policy has the property that whatever the initial state and initial decision are, the remaining decisions must constitute an optimal policy with regard to the state resulting from the first decision". (See Bellman (1957), Chap. III.3., p.83)"

126 We solve the land planner’s problem for every possible initial condition, thus giving rise to general conclusions  
127 on the properties of landscapes and treatments emerging from this problem, under various budget scenarios to  
128 account for climate change.

## 129 2.2 Landscape indicators

130 To characterize the managed landscapes, we mobilize several indicators from landscape ecology and graph theory  
131 (see appendix B). First, we account for the risky and habitat areas in the landscape (eq. B.1). Second, to assess  
132 landscape connectivity/fragmentation and diversity in the context of fire mosaics (Bradstock et al. 2005), we use our  
133 connectivity metric (eq. 2.1), the number of components e.g. the number of maximal connected subgraphs within  
134 the graph, that is not connected to other vertices (eq. B.2) for the risky cells graph, as well as the corresponding  
135 areas. To specifically assess landscape diversity, we use the Simpson index (Simpson 1949) on seral stages (eq.  
136 B.3)<sup>2</sup>. However, the Simpson index does not account for the diversity of spatial patterns: a checkered landscape  
137 with two seral stages would be as diverse as a landscape with two large patches for each seral stage, according to the  
138 Simpson index. Therefore, we use the landscape shape index (eq. B.4), a normalized ratio between the perimeter  
139 of biodiversity habitat and its area (Patton 1975, McGarigal and Marks 1995). To disentangle the correlated effects  
140 of perimeter and area that affect the landscape shape index, we use a land type heterogeneity index, that averages  
141 the probability that, for each cell, neighbors in the 4 cardinal directions share the same land types (eq. B). The  
142 index ranges between 0, when the land type is the same across the whole landscape, to 1, in a checkered landscape.  
143 The index assesses whether the landscape is a mosaic (Bradstock et al. 2005), and if it displays structural diversity,  
144 conducive to diverse communities and functional diversity.

## 145 2.3 Computational experiments

146 Our problem can be viewed as a critical node detection problem, i.e, a problem of locating the nodes that best  
147 degrade connectivity metrics (Arulselvan et al. 2009). Problems of the critical node class are computationally  
148 difficult (e.g. NP - Hard) in a single graph (Arulselvan et al. 2009, Matsypura et al. 2018). Efficient heuristics to  
149 find near-optimal solutions exist and leverage perturbations around local solutions (Arulselvan et al. 2009, Zhou and  
150 Hao 2017). Our problem is a constrained, integer optimization problem that constrains not only the set of nodes  
151 to be removed but also metrics relative to a larger graph structure (e.g. supergraph of risky patches), biodiversity  
152 habitat. For this reason, existing heuristics may not perform well on our problem. Moreover, the complexity of our  
153 combinatorial problem increases with landscape size and vegetation age class exponentially, displaying the ‘curse  
154 of dimensionality’ (Bellman 1957). Therefore, we limit ourselves to studying all the initial conditions in landscapes  
155 of size  $n = 3$  and 4. While this formulation appears simplifying, it encapsulates the main mechanisms displayed

---

<sup>2</sup>Similar results can be found with the Shannon index (Shannon 1948). To avoid issues related to degenerate values and logarithms, we focus on the Simpson index.

156 in similar models (Rachmawati et al. 2016; 2018). It allows us to solve the problem for the whole set of initial  
157 conditions, for the whole range of biodiversity habitat connectivity constraint values, over 20 years. In our analysis,  
158 we consider a range of budget values for treatment costs normalized to 1. As common in the literature, we can  
159 express the budget as a share of land being treated ranging from 5% to 44% of the surface area. These values  
160 encompass historical and projected policies in Australia (Burrows and McCaw 2013), the United States (Office  
161 2019) and Southern Europe (Fernandes et al. 2013).

162 Of all the  $3^{n^2}$  initial conditions landscapes, we only keep landscapes that are unique up to a permutation<sup>3</sup>.  
163 This results in a sharp reduction of landscapes to consider, from 19,683 initial conditions to 2861 unique initial  
164 landscapes for  $n = 3$ , and from 43,046,721 initial to 5,398,082 unique initial landscapes for  $n = 4$ . We focus on  
165 exact optimal solutions for all the initial conditions of these small-scale landscapes and implement our own solution  
166 algorithm in Python 3.9.13. Data and code are publicly available.

## 167 3 Results

### 168 3.1 Steady states

169 Our simulations show that 100% of the initial landscapes converge in finite time towards a steady state solution,  
170 that minimizes wildfire risk while satisfying budgetary and habitat connectivity requirements. Steady states are  
171 landscape cycles with finite periods. Analyzing the steady-state cycles (and the unique landscapes that form them)  
172 drastically reduces the set of landscapes to analyze: they represent 2% (resp. 0.001%) of the initial landscapes of  
173 size  $n = 3$  (resp.  $n = 4$ ). Our model highlights the convergence of landscapes towards types that can be managed  
174 to deliver several objectives. As landscape size increases, the number of steady state landscape cycles increases,  
175 but the power of convergence increases as well (e.g. ratio between initial configurations and effective steady state  
176 landscapes): from 19 683 initial landscapes when  $n = 3$ , 51 steady states emerge and from 43 046 721 initial  
177 landscapes when  $n = 4$ , at most 95 diverse steady-state landscapes emerge. Focusing on steady states makes all  
178 the more sense as landscape size increases.

179 Eventually, figure 2 shows that conditional on data availability on every patch, the more the decision maker  
180 wants to conserve biodiversity, the fewer steady-state landscapes she has to consider. An increase in the habitat  
181 requirement reduces the room for maneuver. Indeed, budget acts as a complexifying factor: the larger the budget  
182 (relative to costs), the larger the set of steady-states to consider. Aiming for relatively large habitat connectivity  
183 reduces the set of viable strategies to be considered and can more efficiently guide policy.

---

<sup>3</sup>That is to say, landscape  $A$  is included in the set of initial conditions  $\mathcal{I}$  if and only if for any element  $B$  in  $\mathcal{I}$ ,  $A$  is not a permutation  
(eg can be obtained through rotations or symmetries) of  $B$

### 184 3.2 Wildfire risk reduction and habitat connectivity in steady state landscapes

185 Figure 3 shows the wildfire risk reductions and habitat requirements normalized by their respective maximum  
186 values for landscapes of size  $n = 3$  and 4. The maximum value for both risk and habitat corresponds to a landscape  
187 covered in 'old' vegetation, which we take to be the counterfactual. Randomly assigned treatments do generate  
188 risk reductions but are not cost nor habitat-efficient. Following our spatial optimization procedure, it is clear that  
189 implementing fuel treatment reduces wildfire risk while supporting biodiversity habitat. Figure 3 shows that these  
190 two objectives come as a trade-off, albeit moderate: indeed, increasing habitat requirements increases the remaining  
191 risk, but there are combinations that can satisfy large habitat connectivity and risk reductions. Budget is a key  
192 factor in risk reduction, as it relaxes the trade-off between the two objectives: increasing the budget reduces the  
193 wildfire risk while maintaining a range of biodiversity constraints. When habitat constraints are large, however,  
194 the marginal effect of budget is limited, and a larger remaining risk needs to be accepted. For example, with a  
195 budget of 25% of land to be treated (with landscape size  $n = 4$ ), and no habitat constraint, risk can be reduced  
196 up to 80% compared to the counterfactual scenario. However, when the habitat constraint is at 60%, only 70% of  
197 risk reduction can be achieved. Moreover, this risk reduction can be achieved with a lower budget. Conversely, as  
198 the costs of treatment increase, for a stable budget, the remaining risk increases sharply, and factoring in habitat  
199 requirements in the decision-making is not necessary for targets below 80%.

### 200 3.3 Properties of steady state landscapes: surface, fragmentation, and diversity

201 Figure 4 displays, for each class, the most frequent steady-state cycle for landscapes of size 3 and 4 for each  
202 biodiversity target. Figure 5 shows the indicators relative to the surface and components of the high-risk graph  
203 and figure 6 shows the indicators related to diversity, both for landscapes of size  $n = 3$  and 4, averaged over all the  
204 steady-state landscape cycles.

205 Previous results show that budget increases risk reduction, conditional on habitat connectivity constraint being  
206 low. Focusing on zones  $A$  and  $A'$  of the panels of figure 5 shows that risk reduction primarily comes from a  
207 reduced surface (panels 5a and 5b), and an increase in the number of components, i.e, disconnected high-risk  
208 patches (panels 5e and 5f). Overall, the high-risk area is reduced and the number of components increases, thus  
209 resulting in smaller largest high-risk component area (panels e and f). As more connected habitat area needs to  
210 be protected, the high-risk surface increases (fig. 4 panels 5a and 5b) and the number of high-risk components  
211 drastically reduces. The landscapes collapse to the same dominant structure (fig. 4), where the high-risk area is  
212 (almost) maximal and there is one large, well-connected component. Overall, landscapes are riskier but also feature  
213 larger, better-connected biodiversity habitat. For large budgets (e.g. 3 and 4), these effects are non-trivial: the  
214 number of components (weakly) increases first, small components either disappear or increase in size (see figure 4  
215 for budget 4 in panels  $A'$ ,  $B'$  and  $C'$ ), risky patches are reallocated to connect separated components before the

216 high-risk surface increases.

217 Landscape diversity unambiguously increases with the budget (panels 6a,6b, sections  $A$  and  $A'$ ). As more units  
218 are treated, the evenness of seral stages increases in the landscapes. When the habitat objective is low, the spatial  
219 diversity of landscapes increases with the budget (panels 6c, 6d): even though the relative area of habitat decreases  
220 with the budget, the shape of habitat is more irregular, and the landscape is more of a mosaic. In this context, cells  
221 with a 'young' seral stage act as stepping stones and corridors between high-risk habitat patches. When habitat  
222 objectives increase, diversity collapses both quantitatively and qualitatively (fig. 6). The Simpson index collapses  
223 from panels  $A$  (resp.  $A'$ ) to  $G$  (resp.  $F'$ ), as land types gradually homogenize (see fig. 4 for an illustration)  
224 across all budgets. Moreover, landscapes form less of a mosaic, and are more clumpy, as displayed by the LSI and  
225 Land type heterogeneity index. Overall, for large habitat targets, landscapes tend to homogenize and to be better  
226 connected, although less quantitatively and qualitatively diverse.

227 Results are consistent across landscape sizes while they display more variability for size  $n = 3$ , as border effects  
228 play a larger role.

### 229 3.4 Spatial allocation of optimal management at the steady-state landscape cycle

230 Figures 7a and 7b display the number of fuel treatments in the steady-state cycles, for various budgets and habitat  
231 connectivity constraints. Treatment allocation follows the evolution of the high-risk area (fig 5a and 5b): the larger  
232 the budget, the larger the treated area, the budget constraint is always satiated. However, when biodiversity targets  
233 increase, the budget constraint is no longer satiated.

234 Figures 7c and 7d display the average spatial location of treatments in the steady state cycles. The darker the  
235 cell, the higher the frequency of treatment. First, not all cells are equally treated. For low levels of biodiversity  
236 constraint, panels  $A$  and  $A'$  of figures 7c and 7d show that central cells are primarily treated, and when the  
237 budget increases, cells on the edges get treated, while corner cells are never treated. In the context of critical node  
238 detection, when the ecological requirements are low, the high-risk graph is primarily considered, and nodes with  
239 the most cost-efficient risk reduction, i.e, with the largest degree are targeted. Once the most connected cells are  
240 treated, lower-degree cells get treated.

241 When habitat constraints increase, several effects come at play. Not only does the number of treatments  
242 decrease, but the spatial allocation also changes. For example, in panels  $A$  and  $B$  for budgets 3 and 4, panels  $C$   
243 and  $D$  for budget 2 and panels  $E$  and  $F$  for budget 1 in figure 7c, the number of treatment remains the same but  
244 is spatially reallocated to lower degree nodes. Treatments are spatially reallocated before being reduced. In this  
245 context, as the relative weight of the habitat graph increases, treating the most cost-efficient risk-reducing nodes  
246 also degrades habitat connectivity. Therefore, as habitat targets increase, edge and corner (e.g. low degree nodes)  
247 are being treated and habitat connectivity is maintained.

## 248 4 Discussion

### 249 4.1 Confirmation and generalization of existing results

250 Our analysis of the exhaustive set of initial conditions for small-scale landscapes confirms existing results in the  
251 literature. We argue that they bring robust evidence and complement the existing literature to derive general  
252 conclusions.

253 Our model encompasses 3 seral stages and 1 composite vegetation type and proves the convergence of every  
254 initial condition to a steady state cycle, irrespective of the initial configuration. We extend [Minas et al. \(2014\)](#)  
255 that find convergence patterns for *homogeneous* landscapes only, i.e, landscapes where the initial vegetation age is  
256 uniformly distributed. We show that in the event of environmental perturbations that do not disrupt ecosystem  
257 dynamics, an appropriate policy can recover the previous equilibrium risk and habitat. We hypothesize that as  
258 long as the risk/ seral-stage relationship reaches a plateau for every vegetation type on the landscape, convergence  
259 should be observed.

260 Our results display a concave production possibility frontier (PPF) between wildfire risk reduction and habitat  
261 connectivity, consistent with PPF literature ([Arthaud and Rose 1996](#), [Calkin et al. 2005](#)). Our results also confirm  
262 that trading one objective for the other is not as efficient as increasing the policy budget to reconcile objectives.  
263 We show that increasing the policy budget nonetheless has diminishing returns for risk reduction, as highlighted  
264 by [Wei et al. \(2008\)](#), [Yemshanov et al. \(2021\)](#) and [Pais et al. \(2021b\)](#).

265 Our study yields clear results in terms of landscape ecology, leveraging concepts from landscape ecology, and  
266 highlighting the spatial mechanisms underlying the shape of PPF. We show that treatment allocation targets the  
267 most central nodes first and then focuses on less connected nodes (e.g cells closer to the border of the landscape)  
268 when habitat goals are low. In doing so, we do find general treatment allocation principles where previous studies  
269 on larger landscapes could not ([Minas et al. 2014](#), [Rachmawati et al. 2016](#)), generalize smaller scale ([Konoshima  
270 et al. 2008](#)) and case study specific ([Yemshanov et al. 2021](#), [Pais et al. 2021a](#)) results.

271 Leveraging a dynamic integer programming, graph theoretic framework on small-scale landscapes, we show that  
272 cell-level metrics help formalize and understand the drivers of treatment allocation and rationalize existing results.  
273 Furthermore, we show that while prioritization approaches based on a graph theoretic framing fare very well in an  
274 unrestricted set-up, including biodiversity habitat targets augments the problem's complexity. We generalize case  
275 studies ([Yemshanov et al. 2022](#)) and show less central high-risk nodes need to be targeted to achieve risk reduction  
276 and safeguard biodiversity habitat.

### 277 4.2 Caveats and methodological perspectives

278 Our analysis tackles the exhaustive set of landscapes of size  $n = 3$  and 4. Our approach allows us to study the  
279 steady-state patterns emerging from any initial condition, replicates existing results in larger landscapes, and sheds

280 light on the mechanisms underlying the wildland dilemma. Increasing landscape size is incompatible with this  
281 approach, as we would run into a dimensionality curse (Bellman 1957). To conserve our exhaustive approach,  
282 different proof mechanisms would be required. Nonetheless, if landscape size is of the essence for actual policy  
283 recommendation, so are other layers of information such as habitat quality, treatment costs, and values at risk  
284 heterogeneity. These other layers would reduce the computational burden, and we believe our results, targeting  
285 the most cost-efficient, risk-reducing, and habitat-conserving strategies, would still apply.

286 In our model, we use a simple relationship to characterize the link between the seral stage, habitat formation  
287 for a single species, and wildfire risk and severity. This choice is motivated by the existence of a lower bound  
288 for a fire return interval and drives our ability to adopt our exhaustive approach. Increasing the number of seral  
289 stages would help to complexify the relationships governing habitat formation and wildfire risk and severity: in  
290 some ecosystems, wildfire risk and severity may be higher for young vegetation than for older and may not be  
291 linear (Taylor et al. 2014). On the other hand, some species may require old-growth forests to survive, not 'young'  
292 forests, and old-growth forests may also be more fire-resilient (Lesmeister et al. 2021). As the number of seral stage  
293 augments, convergence towards steady-state landscape cycles would take longer, but we hypothesize it would still  
294 occur. Moreover, as long as wildfire risk and habitat quality are in conflict, a trade-off would govern treatment  
295 allocation. Multiple seral stages may be targeted for fuel treatment, depending on their location and properties,  
296 but we claim the general mechanism would still apply: in a graph weighted for different risk and habitat properties,  
297 centrality and connectivity would still guide treatment allocation.

298 We implicitly assume that focusing on a given species' habitat would also provide habitat for a variety of  
299 species and be conducive to functional diversity. However, this does not imply that all species would benefit from  
300 maintaining a given habitat type (Saab et al. 2022). Moreover, the lack of structural diversity may cause the trophic  
301 web of the targeted species to collapse. Therefore, management objectives should include structural diversity. In  
302 this case, landscapes could not satisfy extreme habitat connectivity targets and diversity targets. For intermediate  
303 goals, however, we claim that treatment allocation would still aim at fragmenting the landscape, and node centrality  
304 and connectivity would still govern allocation.

305 Eventually, we chose to abstract from a stochastic ignition process affecting the landscape. As a thought  
306 experiment, imagine a Bernoulli-distributed, high-risk area independent probability of ignition in each period. If  
307 part of the landscape ignites, all that remains is the unburnt habitat, while if not, all habitat remains. A decision-  
308 maker faced with maximizing the expected payoff in this scenario would solve the reciprocal of our problem. On  
309 the one hand, she has to ensure that the high-risk cells in the landscape are not 'too' connected, to maximize the  
310 remaining habitat in the event of a wildfire. On the other hand, she wants to maximize connectivity for wildlife  
311 when there is no wildfire. As a result, the trade-off she faces, and the resulting spatial allocation of treatment would  
312 be the same. The stochastic nature of ignition may change the steady state cycles, but convergence would not be  
313 impossible. If the probability of wildfire increases, she focuses more on maintaining a 'young' seral stage over the

314 landscape. In this setting, increasing the probability of ignition would act as a decrease in our habitat target as  
315 well as an increase in the budget available for policy. With our model, we are able to disentangle these two effects  
316 and understand how each constraint would play. We claim we match with actual policy, where the budget is not  
317 fully endogenously determined.

### 318 4.3 Conclusion and policy relevance

319 While there is a *dilemma* for land managers between lowering wildfire risk and severity and maintaining species  
320 habitat connectivity, reconciling the two objectives is not a dead end. This is an important result for land planners  
321 as biodiversity habitat targets are gradually included in policy agendas (for example, the recent pledge by the  
322 participants to the Conference of Parties on Biodiversity in Montreal to preserve 30% of land and oceans by 2030  
323 for biodiversity<sup>4</sup>). It shows that if policymakers can commit to a given budget over time, these biodiversity targets  
324 can be reached and a management cycle that minimizes wildfire risk can be implemented in wildlands. Moreover,  
325 as steady-state cycles are reached, the uncertainty over future land uses is resolved while achieving policy goals.

326 In the face of climate change, treatment costs are expected to increase (Kupfer et al. 2020). The decreasing  
327 marginal efficiency of budget to reduce risk highlights that as climate change increases the costs of treatments, risk,  
328 and damages will increase at an increasing rate, unless the budget is changed accordingly.

329 Our analysis shows that budget should be determined by factoring a careful, *ex-ante* analysis of treatment  
330 costs, the policy maker’s risk aversion towards a measure of wildfire risk and severity, and ecological preferences.  
331 Indeed, low budget-to-cost ratios are incompatible with high risk and severity aversions and/or large ecological  
332 requirements.

333 As wildfires and biodiversity habitat destruction are challenges in the face of global warming, finding policy  
334 guidance tools is of the essence. Many studies focus on specific case studies or limited ranges of potential initial  
335 conditions. We develop a simplified ecological model of habitat and wildfire connectivity to guide policymakers in  
336 the form of general principles. Reducing wildfire risk and accommodating wildlife habitat is possible with carefully  
337 designed policies, where budget plays a key role. However, it is impossible to achieve drastic risk reduction without  
338 harming biodiversity habitat. General principles of treatment allocation in the landscape are derived, and the  
339 concepts of graph theory provide an operational toolbox to understand the underlying mechanisms. Landscape  
340 patches that display high wildfire risk seral stages and are well connected to other patches should be treated first.  
341 When habitat targets are included, tackling lower-risk patches is of the essence to maintain habitat connectivity.

342 Our article summarizes and generalizes how policies should be implemented, both in terms of budgets and  
343 spatial allocation, to protect and enhance ecosystem health.

---

<sup>4</sup>See Target 2 in the [Keunming-Montreal Global Diversity Framework, 2022](#)

## 344 **5 Declaration**

### 345 **5.1 Acknowledgments**

346 This research was conducted while SJ was on leave at the Environmental Markets Lab, UC Santa Barbara. We  
347 acknowledge support from the Center for Scientific Computing from the CNSI, MRL: an NSF MRSEC (DMR-  
348 1720256) and NSF CNS- 1725797, at UC Santa Barbara. Moreover, the authors are grateful to the editor and  
349 X anonymous referees, as well as participants to the Columbia Interdisciplinary PhD Workshop in Sustainable  
350 Development and the BINGO group at CIRED for their valuable comments.

### 351 **5.2 Data availability**

352 Given its size, steady-state cycle data is available upon request from the authors. Code for replication is available  
353 at [https://github.com/sim-jean/Landscape\\_connectivity\\_dilemma](https://github.com/sim-jean/Landscape_connectivity_dilemma)

### 354 **5.3 Author affiliation**

355 CIRED, Ecole des Ponts, AgroParisTech, EHESS, CIRAD, CNRS, Université Paris-Saclay, Nogent-sur-Marne,  
356 France

### 357 **5.4 Competing interests**

358 The authors declare no conflict of interest.

### 359 **5.5 Contribution**

360 LM designed the study, SJ ran the computational experiment, SJ and LM analyzed the results and wrote the  
361 manuscript.

## 362 Appendix

### 363 A Theoretical model

#### 364 A.1 Vegetation dynamics

365 In cell  $i$  at time  $t$ , vegetation ages  $A_i(t)$  evolves according to the following :

$$A_i(t+1) = (A_i(t) + 1)(1 - x_i(t)), t \in \{0, 1, \dots, T\}, \forall i \in C \quad (\text{A.1})$$

366 Where  $x_i(t) \in \{0, 1\}$  is a binary variable, representing the treatment status of cell  $i$  at time  $t$ . Correspondingly,  
367 the age vector across the landscape is  $A(t) = \{A_i(t)\}_{i \in C}$ .

#### 368 A.2 Mature habitat and risky patch designation

369 Cell  $i$  is labeled 'mature' to host wildlife in year  $t$  as:

$$Mature_i(A(t)) = \begin{cases} 1 & \text{if } A_i(t) \geq m \\ 0 & \text{otherwise} \end{cases} \quad (\text{A.2})$$

370 Where  $m$  is the 'mature' threshold. Correspondingly, the vector of mature cells across the landscape is  $Mature(A(t)) =$   
371  $\{Mature_i(A(t))\}_{i \in C}$

372 Similarly, cell  $i$  is labeled as 'high fuel load' in year  $t$  as:

$$High_i(A(t)) = \begin{cases} 1 & \text{if } A_i(t) \geq d \\ 0 & \text{otherwise} \end{cases} \quad (\text{A.3})$$

373 Where  $d$  is the 'high fuel load' threshold. Correspondingly, the vector of high fuel load cells across the landscape  
374 is  $High(A(t)) = \{High_i(A(t))\}_{i \in C}$

375 We assume that the maturity threshold is crossed before the high risk threshold, i.e  $m < d$ .

#### 376 A.3 Global connectivity index and graph theory

377 Let a grided landscape of size  $n$ , where for each cell  $a_i$  in the set of cells  $A$  in the landscape, one defines  $\Phi_i$  the set  
378 of cells connected to cell  $i$  (i.e, cells share the same status and can only be in the 8-direction direct neighborhood).

379 Moreover, let  $Q_{ij}$  be a binary variable such that  $Q_{ij} = 1$  if cells  $a_i$  and  $a_j$  are connected, 0 otherwise. [Minas et al.](#)  
380 (2014) define the following connectivity metric over a landscape:

$$\sum_{i \in C} \sum_{j \in \Phi_i} Q_{ij} \quad (\text{A.4})$$

381 Now view the landscape as a graph  $G$ , with vertices  $V$  and edges  $E$  such that  $G(V, E)$ . For the proof, assume  
 382 that  $Y$  is a binary vector such that  $Y_i = 1$  if cell  $i$  is 'high risk' and 0 otherwise, and that we focus on the 'high  
 383 risk' graph on the landscape. The argument is identical in the case of mature habitat.

384 In graph theory, an adjacency matrix  $\mathcal{K}$  for an undirected graph is a binary, symmetric, square matrix of  
 385 dimension  $\text{card}(V)^2$  where  $k_{ij} = 1$  if vertices  $i$  and  $j$  are connected, 0 otherwise. In our context, it is clear that  
 386  $k_{ij} = Q_{ij}$ . Equation A.4 can be reformulated as :

$$Y' \mathcal{K} Y = \sum_j \left( Y_j \sum_i Y_i k_{ij} \right) = \sum_j \left( Y_j \left( Y_j k_{jj} + \sum_{i \neq j} Y_i k_{ij} \right) \right)$$

387 Given the symmetric nature of  $\mathcal{K}$ ,  $\forall i \neq j$ ,  $k_{ij} = k_{ji}$ . Each cell is connected to itself so  $k_{jj} = 1$ .  $Y_i \in \{0, 1\}$  i.e  
 388  $Y_i^2 \in \{0, 1\}$ :

$$\begin{aligned} Y' \mathcal{K} Y &= \sum_j \left( Y_j^2 + \sum_{i \neq j} Y_i Y_j k_{ij} \right) \\ &= \sum_j Y_j + 2 \sum_{j < i} \left( \sum_{i \neq j} Y_j Y_i a_{ij} \right) \end{aligned}$$

389 The first sum is the number of cells either 'mature' or 'high risk', i.e, the cardinal of the nodes of the 'high risk'  
 390 graph e.g  $\text{card}(V)$ . In the second sum,  $\sum_{i \neq j} Y_j Y_i a_{ij}$  is the number of connections of cell  $i$  to cell  $j$ , as the product  
 391  $Y_i Y_j a_{ij} = 1$  if and only if cell  $i$  and  $j$  share the same status ( $Y_i = Y_j$ ) and are in the 8-cell neighborhood ( $a_{ij} = 1$ ).  
 392 By definition, the sum of the number of connections of each cell to other cells is  $\text{card}(E)$ . Hence, for a set of cells  
 393  $C$ , reformulated in terms of graph theory :

$$\sum_{i \in C} \sum_{j \in \Phi_i} Q_{ij} = \text{card}(V) + 2\text{card}(E) \quad (\text{A.5})$$

#### 394 A.4 Dynamic programming equation

395 The Bellman equation links current and future payoffs in a recurring fashion.

$$V(t, A) = \min_{x \in \{0, 1\}^{n^2}} (H(A) + V(t + 1, A_t + 1)) \quad (\text{A.6})$$

396 subject to constraints (2.3), (2.5), (2.4) and (2.7).

397 We use backward induction given by the final value  $V(T, A) = H(A)$  to dynamically solve the program.

## 398 B Landscape indicators

399 **Area** We use the number of vertices (nodes) for both subgraphs and take into account cell dimensions:

$$Area(G_i) = card(V_i) \text{ for } i \in \{B, F\} \quad (\text{B.1})$$

### Number of components

$$\#components_i = card(\text{Maximal connected subgraphs of } G_i \text{ for } i \in \{B, F\}) \quad (\text{B.2})$$

400 **Simpson diversity index:** let  $p_i$  be the proportion of land type  $i$  in the landscape. The Simpson diversity index  
401 is :

$$SIDI = 1 - \sum_i p_i^2 \quad (\text{B.3})$$

402 **Landscape shape index:** following McGarigal and Marks (1995), the adapted LSI index from Patton (1975) in  
403 a raster landscape is:

$$LSI = \frac{0.25 \times perimeter(G)}{n} \quad (\text{B.4})$$

404 Where  $perimeter(G)$  is the perimeter of the cells comprised in the graph as vertices.

405 **Land Type Heterogeneity Index:** let  $d_{ij}$  be a binary variable such that  $d_{ij} = 1$  if patch  $i$  and  $j$  share the  
406 same land type. Define  $\mathcal{J}$  as the set of neighbors in 4 directions (north, south, east, west) of cell  $i$ <sup>5</sup>. The land type  
407 heterogeneity index is :

$$LTH = \frac{1}{N} \sum_{i=1}^N \left( \frac{\sum_{j \in \mathcal{J}_i} d_{ij}}{card(\mathcal{J}_i)} \right) \quad (\text{B.5})$$

408

---

<sup>5</sup>The set  $\mathcal{J}_i$  varies with cell  $i$  to account for edge effects

## References

- John T. Abatzoglou and A. Park Williams. Impact of anthropogenic climate change on wildfire across western us forests. *Proceedings of the National Academy of Sciences*, 113(42):11770–11775, 2016. doi: 10.1073/pnas.1607171113. URL <https://www.pnas.org/doi/abs/10.1073/pnas.1607171113>.
- Greg J. Arthaud and Dietmar W. Rose. A methodology for estimating production possibility frontiers for wildlife habitat and timber value at the landscape level. *Canadian Journal of Forest Research*, 26(12):2191–2200, December 1996. ISSN 0045-5067. doi: 10.1139/x26-248. URL <https://cdnsiencepub.com/doi/10.1139/x26-248>. Publisher: NRC Research Press.
- Ashwin Arulselvan, Clayton W. Commander, Lily Eleftheriadou, and Panos M. Pardalos. Detecting critical nodes in sparse graphs. *Computers Operations Research*, 36(7):2193–2200, 2009. ISSN 0305-0548. doi: <https://doi.org/10.1016/j.cor.2008.08.016>. URL <https://www.sciencedirect.com/science/article/pii/S0305054808001494>.
- Richard Bellman. *Dynamic Programming*. Princeton University Press, 1957.
- Matthias M. Boer, Rohan J. Sadler, Roy S. Wittkuhn, Lachlan McCaw, and Pauline F. Grierson. Long-term impacts of prescribed burning on regional extent and incidence of wildfires—Evidence from 50 years of active fire management in SW Australian forests. *Forest Ecology and Management*, 259(1):132–142, 2009. ISSN 0378-1127. doi: <https://doi.org/10.1016/j.foreco.2009.10.005>. URL <https://www.sciencedirect.com/science/article/pii/S0378112709007294>.
- S. D. Bradshaw, K.W. Dixon, H. Lambers, A.T. Cross, J. Bailey, and S.D. Hopper. Understanding the long-term impact of prescribed burning in mediterranean-climate biodiversity hotspots, with a focus on south-western australia. *International Journal of Wildland Fire*, 27, 2018.
- R. A. Bradstock, M. Bedward, A. M. Gill, J. S. Cohn, R. A. Bradstock, M. Bedward, A. M. Gill, and J. S. Cohn. Which mosaic? A landscape ecological approach for evaluating interactions between fire regimes, habitat and animals. *Wildlife Research*, 32(5): 409–423, August 2005. ISSN 1448-5494, 1448-5494. doi: 10.1071/WR02114. URL <https://www.publish.csiro.au/wr/WR02114>.
- Marshall Burke, Marissa L. Childs, Brandon De la Cuesta, Minghao Qiu, Jessica Li, Carlos F. Gould, Sam Heft-Neal, and Michael Wara. Wildfire Influence on Recent US Pollution Trends, January 2023. URL <https://www.nber.org/papers/w30882>.
- Neil Burrows and Lachlan McCaw. Prescribed burning in southwestern australian forests. *Frontiers in Ecology and the Environment*, 11(s1):e25–e34, 2013. doi: <https://doi.org/10.1890/120356>. URL <https://esajournals.onlinelibrary.wiley.com/doi/abs/10.1890/120356>.
- David E Calkin, Susan Stevens Hummel, and James K Agee. Modeling trade-offs between fire threat reduction and late-seral forest structure. *Canadian Journal of Forest Research*, 35(11):2562–2574, November 2005. ISSN 0045-5067. doi: 10.1139/x05-177. URL <https://cdnsiencepub.com/doi/10.1139/x05-177>. Publisher: NRC Research Press.
- Jonathan D Coop, Sean A Parks, Camille S Stevens-Rumann, Shelley D Crausbay, Philip E Higuera, Matthew D Hurteau, Alan Tepley, Ellen Whitman, Timothy Assal, Brandon M Collins, Kimberley T Davis, Solomon Dobrowski, Donald A Falk, Paula J Fornwalt, Peter Z Fulé, Brian J Harvey, Van R Kane, Caitlin E Littlefield, Ellis Q Margolis, Malcolm North, Marc-André Parisien, Susan Prichard, and Kyle C Rodman. Wildfire-Driven Forest Conversion in Western North American Landscapes. *BioScience*, 70(8): 659–673, August 2020. ISSN 0006-3568. doi: 10.1093/biosci/biaa061. URL <https://doi.org/10.1093/biosci/biaa061>.
- Lenore Fahrig, Jacques Baudry, Lluís Brotons, Françoise G. Burel, Thomas O. Crist, Robert J. Fuller, Clelia Sirami, Gavin M. Siriwardena, and Jean-Louis Martin. Functional landscape heterogeneity and animal biodiversity in agricultural landscapes. *Ecology Letters*, 14(2):101–112, 2011. doi: <https://doi-org.inshs.bib.cnrs.fr/10.1111/j.1461-0248.2010.01559.x>. URL <https://onlinelibrary-wiley-com.inshs.bib.cnrs.fr/doi/abs/10.1111/j.1461-0248.2010.01559.x>.

447 Paulo M Fernandes, G Matt Davies, Davide Ascoli, Cristina Fernández, Francisco Moreira, Eric Rigolot, Cathelijne R Stoof,  
448 José Antonio Vega, and Domingo Molina. Prescribed burning in southern europe: developing fire management in a dy-  
449 namic landscape. *Frontiers in Ecology and the Environment*, 11(s1):e4–e14, 2013. doi: <https://doi.org/10.1890/120298>. URL  
450 <https://esajournals.onlinelibrary.wiley.com/doi/abs/10.1890/120298>.

451 Mark A. Finney. Design of Regular Landscape Fuel Treatment Patterns for Modifying Fire Growth and Behavior. *Forest Science*, 47  
452 (2):219–228, May 2001. ISSN 0015-749X. doi: 10.1093/forestscience/47.2.219. URL <https://doi.org/10.1093/forestscience/47.2.219>.

453

454 Mark A. Finney. A computational method for optimising fuel treatment locations. *International Journal of Wildland Fire*, 16(6):  
455 702–711, December 2007. ISSN 1448-5516, 1448-5516. doi: 10.1071/WF06063. URL <https://www.publish.csiro.au/wf/WF06063>.  
456 Publisher: CSIRO PUBLISHING.

457 Veronique Florec, Michael Burton, David Pannell, Joel Kelso, and George Milne. Where to prescribe burn: the costs and benefits of  
458 prescribed burning close to houses. *International Journal of Wildland Fire*, (29), 2020.

459 Jacob Gellman, Margaret Walls, and Matthew Wibbenmeyer. Welfare losses from wildfire smoke: evidence from daily outdoor recreation  
460 data. *Resources for the Future Working Papers*, 2023.

461 Jose Ramon Gonzalez-Olabarria, Jaime Carrasco, Cristobal Pais, Jordi Garcia-Gonzalo, David Palacios-Meneses, Rodrigo Mahaluf-  
462 Recasens, Olena Porkhum, and Andrés Weintraub. A fire spread simulator to support tactical management decisions for Mediter-  
463 ranean landscapes. *Frontiers in Forests and Global Change*, 6, 2023. ISSN 2624-893X. URL [https://www.frontiersin.org/](https://www.frontiersin.org/articles/10.3389/ffgc.2023.1071484)  
464 [articles/10.3389/ffgc.2023.1071484](https://www.frontiersin.org/articles/10.3389/ffgc.2023.1071484).

465 Sam Heft-Neal, Carlos F. Gould, Marissa Childs, Mathew V. Kiang, Kari Nadeau, Mark Duggan, Eran Bendavid, and Marshall Burke.  
466 Behavior Mediates the Health Effects of Extreme Wildfire Smoke Events, February 2023. URL [https://www.nber.org/papers/](https://www.nber.org/papers/w30969)  
467 [w30969](https://www.nber.org/papers/w30969).

468 W. Matt Jolly, Mark A. Cochrane, Patrick H. Freeborn, Zachary A. Holden, Timothy J. Brown, Grant J. Williamson, and David M.  
469 J. S. Bowman. Climate-induced variations in global wildfire danger from 1979 to 2013. *Nature Communications*, 6(1):7537, July  
470 2015. ISSN 2041-1723. doi: 10.1038/ncomms8537. URL <https://doi.org/10.1038/ncomms8537>.

471 Elizabeth L. Kalies and Larissa L. Yocom Kent. Tamm review: Are fuel treatments effective at achieving ecological and social objectives?  
472 a systematic review. *Forest Ecology and Management*, 375:84–95, 2016. ISSN 0378-1127. doi: [https://doi.org/10.1016/j.foreco.2016.](https://doi.org/10.1016/j.foreco.2016.05.021)  
473 [05.021](https://doi.org/10.1016/j.foreco.2016.05.021). URL <https://www.sciencedirect.com/science/article/pii/S0378112716302626>.

474 Masashi Konoshima, Claire A. Montgomery, Heidi J. Albers, and Jeffrey L. Arthur. Spatial-Endogenous Fire Risk and Efficient Fuel  
475 Management and Timber Harvest. *Land Economics*, 84(3):449–468, August 2008. ISSN 0023-7639, 1543-8325. doi: 10.3368/le.84.3.  
476 449. URL <https://le.uwpress.org/content/84/3/449>. Publisher: University of Wisconsin Press Section: Articles.

477 J.A Kupfer, A. Terando, P. Gao, C. Teske, and J.K. Hiern. Climate change projected to reduce prescribed burning opportunities in the  
478 south-eastern united states. *International Journal of Wildland Fire*, 29, 2020.

479 John F. Lehmkuhl, Maureen Kennedy, E. David Ford, Peter H. Singleton, William L. Gaines, and Rick L. Lind. Seeing the forest for the  
480 fuel: Integrating ecological values and fuels management. *Forest Ecology and Management*, 246(1):73–80, 2007. ISSN 0378-1127. doi:  
481 <https://doi.org/10.1016/j.foreco.2007.03.071>. URL <https://www.sciencedirect.com/science/article/pii/S0378112707002800>.

482 Damon B. Lesmeister, Raymond J. Davis, Stan G. Sovern, and Zhiqiang Yang. Northern spotted owl nesting forests as fire refugia: a  
483 30-year synthesis of large wildfires. *Fire Ecology*, 17(1):32, November 2021. ISSN 1933-9747. doi: 10.1186/s42408-021-00118-z. URL  
484 <https://doi.org/10.1186/s42408-021-00118-z>.

485 Susan C. Loeb and Rachel V. Blakey. Bats and fire: a global review. *Fire Ecology*, 17(1):29, November 2021. ISSN 1933-9747. doi:  
486 10.1186/s42408-021-00109-0. URL <https://doi.org/10.1186/s42408-021-00109-0>.

487 Kathryn E. Low, John J. Battles, Ryan E. Tompkins, Colin P. Dillingham, Scott L. Stephens, and Brandon M. Collins. Shaded fuel  
488 breaks create wildfire-resilient forest stands: lessons from a long-term study in the Sierra Nevada. *Fire Ecology*, 19(1):29, May 2023.  
489 ISSN 1933-9747. doi: 10.1186/s42408-023-00187-2. URL <https://doi.org/10.1186/s42408-023-00187-2>.

490 Dmytro Matsypura, Oleg A. Prokopyev, and Aizat Zahar. Wildfire fuel management: Network-based models and optimization of  
491 prescribed burning. *European Journal of Operational Research*, 264(2):774–796, January 2018. ISSN 03772217. doi: 10.1016/j.ejor.  
492 2017.06.050. URL <https://linkinghub.elsevier.com/retrieve/pii/S037722171730591X>.

493 Michael A. McCarthy, A. Malcolm Gill, and Ross A. Bradstock. Theoretical fire-interval distributions. *International Journal of*  
494 *Wildland Fire*, 10(1):73–77, 2001. URL <https://doi.org/10.1071/WF01013>.

495 Kevin McGarigal and Barbara J. Marks. FRAGSTATS: spatial pattern analysis program for quantifying landscape structure. Technical  
496 report, 1995. URL <https://doi.org/10.2737%2Fpnw-gtr-351>.

497 James Minas, John W. Hearne, and David L. Martell. A spatial optimisation model for multi-period landscape level fuel management  
498 to mitigate wildfire impacts. *European Journal of Operational Research*, 232(2):412–422, January 2014. ISSN 0377-2217. doi:  
499 10.1016/j.ejor.2013.07.026. URL <https://www.sciencedirect.com/science/article/pii/S0377221713006073>. Publisher: North-  
500 Holland.

501 Emily S. Minor and Dean L. Urban. A Graph-Theory Framework for Evaluating Landscape Connectivity and Conservation Planning.  
502 *Conservation Biology*, 22(2):297–307, 2008. ISSN 1523-1739. doi: 10.1111/j.1523-1739.2007.00871.x. URL <http://onlinelibrary.wiley.com/doi/abs/10.1111/j.1523-1739.2007.00871.x>. eprint: <https://conbio.onlinelibrary.wiley.com/doi/pdf/10.1111/j.1523-1739.2007.00871.x>.

503 <http://onlinelibrary.wiley.com/doi/abs/10.1111/j.1523-1739.2007.00871.x>. eprint: <https://conbio.onlinelibrary.wiley.com/doi/pdf/10.1111/j.1523-1739.2007.00871.x>.

504 1739.2007.00871.x.

505 L. Mouysset, L. Doyen, and F. Jiguet. How does economic risk aversion affect biodiversity? *Ecological Applications*, 23(1):96–109,  
506 2013. ISSN 10510761. URL <http://www.jstor.org/stable/23440820>.

507 United States Government Accountability Office. Wildland fire - federal agencies' efforts to reduce wildland fuels and lower risk to  
508 communities and ecosystems. Technical report, United States Government Accountability Office, 2019.

509 Andrew D. Olds, Kylie A. Pitt, Paul S. Maxwell, and Rod M. Connolly. Synergistic effects of reserves and connectivity on ecological  
510 resilience. *Journal of Applied Ecology*, 49(6):1195–1203, 2012. doi: <https://doi.org/10.1111/jpe.12002>. URL <https://besjournals.onlinelibrary.wiley.com/doi/abs/10.1111/jpe.12002>.

511 <https://besjournals.onlinelibrary.wiley.com/doi/abs/10.1111/jpe.12002>.

512 Jerry S. Olson. Energy storage and the balance of producers and decomposers in ecological systems. *Ecology*, 44(2):322–331, 1963.  
513 doi: <https://doi-org.inshs.bib.cnrs.fr/10.2307/1932179>. URL <https://esajournals-onlinelibrary-wiley-com.inshs.bib.cnrs.fr/doi/abs/10.2307/1932179>.

514 <https://esajournals-onlinelibrary-wiley-com.inshs.bib.cnrs.fr/doi/abs/10.2307/1932179>.

515 Cristobal Pais, Jaime Carrasco, Pelagie Elimbi Moudio, and Zuo-Jun Max Shen. Downstream protection value: Detecting critical  
516 zones for effective fuel-treatment under wildfire risk. *Computers & Operations Research*, 131, July 2021a. ISSN 0305-0548. doi:  
517 10.1016/j.cor.2021.105252. URL <https://www.sciencedirect.com/science/article/pii/S0305054821000447>.

518 Cristobal Pais, Jaime Carrasco, David L. Martell, Andres Weintraub, and David L. Woodruff. Cell2Fire: A Cell-Based Forest Fire  
519 Growth Model to Support Strategic Landscape Management Planning. *Frontiers in Forests and Global Change*, 4, 2021b. ISSN  
520 2624-893X. URL <https://www.frontiersin.org/articles/10.3389/ffgc.2021.692706>.

521 Lucía Pascual-Hortal and Santiago Saura. Comparison and development of new graph-based landscape connectivity indices: towards  
522 the prioritization of habitat patches and corridors for conservation. *Landscape Ecology*, 21(7):959–967, October 2006. ISSN 0921-2973,  
523 1572-9761. doi: 10.1007/s10980-006-0013-z. URL <http://link.springer.com/10.1007/s10980-006-0013-z>.

524 David R. Patton. A Diversity Index for Quantifying Habitat "Edge". *Wildlife Society Bulletin (1973-2006)*, 3(4):171–173, 1975. ISSN  
525 0091-7648. URL <https://www.jstor.org/stable/3781151>. Publisher: [Wiley, Wildlife Society].

526 Seth H. Peterson, Marco E. Morais, Jean M. Carlson, Philip E. Dennison, Dar A. Roberts, Max A. Moritz, and David R. Weise. Using  
527 HFire for spatial modeling of fire in shrublands. Technical report, 2009. URL <https://doi.org/10.2737/2Fpaw-rp-259>.

528 Ramya Rachmawati, Melih Ozlen, Karin J. Reinke, and John W. Hearne. A model for solving the prescribed burn planning prob-  
529 lem. *SpringerPlus*, 4(1):630, October 2015. ISSN 2193-1801. doi: 10.1186/s40064-015-1418-4. URL <https://doi.org/10.1186/s40064-015-1418-4>.

530

531 Ramya Rachmawati, Melih Ozlen, Karin J. Reinke, and John W. Hearne. An optimisation approach for fuel treatment planning  
532 to break the connectivity of high-risk regions. *Forest Ecology and Management*, 368:94–104, May 2016. ISSN 0378-1127. doi:  
533 10.1016/j.foreco.2016.03.014. URL <https://www.sciencedirect.com/science/article/pii/S0378112716300731>.

534 Ramya Rachmawati, Melih Ozlen, John Hearne, and Karin Reinke. Fuel treatment planning: Fragmenting high fuel load areas while  
535 maintaining availability and connectivity of faunal habitat. *Applied Mathematical Modelling*, 54:298–310, February 2018. ISSN  
536 0307-904X. doi: 10.1016/j.apm.2017.09.045. URL <https://www.sciencedirect.com/science/article/pii/S0307904X17306066>.

537 Bronwyn Rayfield, David Pelletier, Maria Dumitru, Jeffrey A. Cardille, and Andrew Gonzalez. Multipurpose habitat networks for short-  
538 range and long-range connectivity: a new method combining graph and circuit connectivity. *Methods in Ecology and Evolution*, 7(2):  
539 222–231, February 2016. ISSN 2041-210X. URL <https://onlinelibrary.wiley.com/doi/abs/10.1111/2041-210X.12470>. Publisher:  
540 John Wiley & Sons, Ltd.

541 Julien Ruffault, Thomas Curt, Nicolas K. Martin-StPaul, Vincent Moron, and Ricardo M. Trigo. Extreme wildfire events are linked  
542 to global-change-type droughts in the northern Mediterranean. *Natural Hazards and Earth System Sciences*, 18(3):847–856, March  
543 2018. ISSN 1561-8633. doi: 10.5194/nhess-18-847-2018. URL <https://nhess.copernicus.org/articles/18/847/2018/>. Publisher:  
544 Copernicus GmbH.

545 Adam Rytwinski and Kevin A. Crowe. A simulation-optimization model for selecting the location of fuel-breaks to minimize expected  
546 losses from forest fires. *Forest Ecology and Management*, 260(1):1–11, June 2010. ISSN 0378-1127. doi: 10.1016/j.foreco.2010.03.013.  
547 URL <https://www.sciencedirect.com/science/article/pii/S0378112710001593>.

548 Victoria A. Saab, Quresh R. Latif, William M. Block, and Jonathan G. Dudley. Short-term benefits of prescribed fire to bird communities  
549 of dry forests. *Fire Ecology*, 18(1):4, April 2022. ISSN 1933-9747. doi: 10.1186/s42408-022-00130-x. URL <https://doi.org/10.1186/s42408-022-00130-x>.

550

551 C. E. Shannon. A mathematical theory of communication. *Bell System Technical Journal*, 27(3):379–423, 1948. doi: <https://doi.org/10.1002/j.1538-7305.1948.tb01338.x>. URL <https://onlinelibrary.wiley.com/doi/abs/10.1002/j.1538-7305.1948.tb01338.x>.

552

553 E. H. Simpson. Measurement of Diversity. *Nature*, 163(4148):688–688, April 1949. ISSN 1476-4687. doi: 10.1038/163688a0. URL  
554 <https://doi.org/10.1038/163688a0>.

555 Holly Sitters, Julian Di Stefano, Fiona J. Christie, Paul Sunnucks, and Alan York. Bird diversity increases after patchy prescribed  
556 fire: implications from a before-after control-impact study. *International Journal of Wildland Fire*, 24:690–701, 2015. URL <https://api.semanticscholar.org/CorpusID:129053082>.

557

558 Kristin Sweeney, Ruth Dittrich, Spencer Moffat, Chelsea Power, and Jeffrey D. Kline. Estimating the economic value of carbon losses  
559 from wildfires using publicly available data sources: Eagle Creek Fire, Oregon 2017. *Fire Ecology*, 19(1):55, September 2023. ISSN  
560 1933-9747. doi: 10.1186/s42408-023-00206-2. URL <https://doi.org/10.1186/s42408-023-00206-2>.

561 Chris Taylor, Michael A. McCarty, and David B. Lindemayer. Nonlinear effects of stand age on fire severity. *Conservation Letters*,  
562 (7), 2014. doi: doi:10.1111/conl.12122.

563 Philip D. Taylor, Lenore Fahrig, Kringen Henein, and Gray Merriam. Connectivity is a vital element of landscape structure. *Oikos*, 68  
564 (3):571–573, 1993. ISSN 00301299, 16000706. URL <http://www.jstor.org/stable/3544927>.

565 Alan R Templeton, Hilary Brazeal, and Jennifer L Neuwald. The transition from isolated patches to a metapopulation in the eastern  
566 collared lizard in response to prescribed fires. *Ecology*, 92(9):1736–1747, 2011. doi: <https://doi.org/10.1890/10-1994.1>. URL  
567 <https://esajournals.onlinelibrary.wiley.com/doi/abs/10.1890/10-1994.1>.

568 Yuhong Tian, Yiqing Liu, C. Y. Jim, and Hanzhang Song. Assessing Structural Connectivity of Urban Green Spaces in Metropolitan  
569 Hong Kong. *Sustainability*, 9(9):1653, September 2017. ISSN 2071-1050. doi: 10.3390/su9091653. URL [https://www.mdpi.com/](https://www.mdpi.com/2071-1050/9/9/1653)  
570 [2071-1050/9/9/1653](https://www.mdpi.com/2071-1050/9/9/1653). Number: 9.

571 Monica G. Turner. Landscape ecology: What is the state of the science? *Annual Review of Ecology, Evolution, and Systematics*, 36  
572 (1):319–344, 2005. doi: 10.1146/annurev.ecolsys.36.102003.152614. URL [https://doi.org/10.1146/annurev.ecolsys.36.102003.](https://doi.org/10.1146/annurev.ecolsys.36.102003.152614)  
573 [152614](https://doi.org/10.1146/annurev.ecolsys.36.102003.152614).

574 Monica G. Turner and Robert H. Gardner. *Landscape Ecology in Theory and Practice*. Springer New York, 2015.

575 Dean Urban and Timothy Keitt. Landscape Connectivity: A Graph-Theoretic Perspective. *Ecology*, 82(5):1205–1218, 2001. ISSN  
576 1939-9170. doi: 10.1890/0012-9658(2001)082[1205:LCAGTP]2.0.CO;2. URL [https://onlinelibrary.wiley.com/doi/abs/10.1890/](https://onlinelibrary.wiley.com/doi/abs/10.1890/0012-9658%282001%29082%5B1205%3ALCAGTP%5D2.0.CO%3B2)  
577 [0012-9658%282001%29082%5B1205%3ALCAGTP%5D2.0.CO%3B2](https://onlinelibrary.wiley.com/doi/abs/10.1890/0012-9658%282001%29082%5B1205%3ALCAGTP%5D2.0.CO%3B2).

578 Nicole Vaillant, Jo Ann Fites-Kaufman, and Scott L. Stephens. Effectiveness of prescribed fire as a fuel treatment in californian  
579 coniferous forests. *International Journal of Wildland Fire*, (18), 2009.

580 J. Velázquez, J. Gutiérrez, A. García-Abril, A. Hernando, M. Aparicio, and B. Sánchez. Structural connectivity as an indicator of species  
581 richness and landscape diversity in Castilla y León (Spain). *Forest Ecology and Management*, 432:286–297, 2019. ISSN 0378-1127. doi:  
582 <https://doi.org/10.1016/j.foreco.2018.09.035>. URL <https://www.sciencedirect.com/science/article/pii/S0378112718312957>.

583 Daoping Wang, Dabo Guan, Shupeng Zhu, Michael Mac Kinnon, Guannan Geng, Qiang Zhang, Heran Zheng, Tianyang Lei, Shuai  
584 Shao, Peng Gong, and Steven J. Davis. Economic footprint of California wildfires in 2018. *Nature Sustainability*, 4(3):252–260,  
585 March 2021. ISSN 2398-9629. doi: 10.1038/s41893-020-00646-7. URL <https://doi.org/10.1038/s41893-020-00646-7>.

586 Tzeidle N. Wasserman and Stephanie E. Mueller. Climate influences on future fire severity: a synthesis of climate-fire interactions  
587 and impacts on fire regimes, high-severity fire, and forests in the western United States. *Fire Ecology*, 19(1):43, July 2023. ISSN  
588 1933-9747. doi: 10.1186/s42408-023-00200-8. URL <https://doi.org/10.1186/s42408-023-00200-8>.

589 Yu Wei, Douglas Rideout, and Andy Kirsch. An optimization model for locating fuel treatments across a landscape to reduce expected  
590 fire losses. *Canadian Journal of Forest Research*, 38(4):868–877, April 2008. ISSN 0045-5067. doi: 10.1139/X07-162. URL  
591 <https://cdnsiencepub.com/doi/10.1139/X07-162>. Publisher: NRC Research Press.

592 Brooke A. Williams, Luke P. Shoo, Kerrie A. Wilson, and Hawthorne L. Beyer. Optimising the spatial planning of prescribed burns  
593 to achieve multiple objectives in a fire-dependent ecosystem. *Journal of Applied Ecology*, 54(6):1699–1709, 2017. doi: <https://doi.org/10.1111/1365-2664.12920>. URL  
594 <https://besjournals.onlinelibrary.wiley.com/doi/abs/10.1111/1365-2664.12920>.

595 Brendan A. Wintle, Sarah Legge, and John C.Z. Woinarski. After the megafires: What next for australian wildlife? *Trends in*  
596 *Ecology Evolution*, 35(9):753–757, 2020. ISSN 0169-5347. doi: <https://doi.org/10.1016/j.tree.2020.06.009>. URL <https://www.sciencedirect.com/science/article/pii/S0169534720301713>.  
597

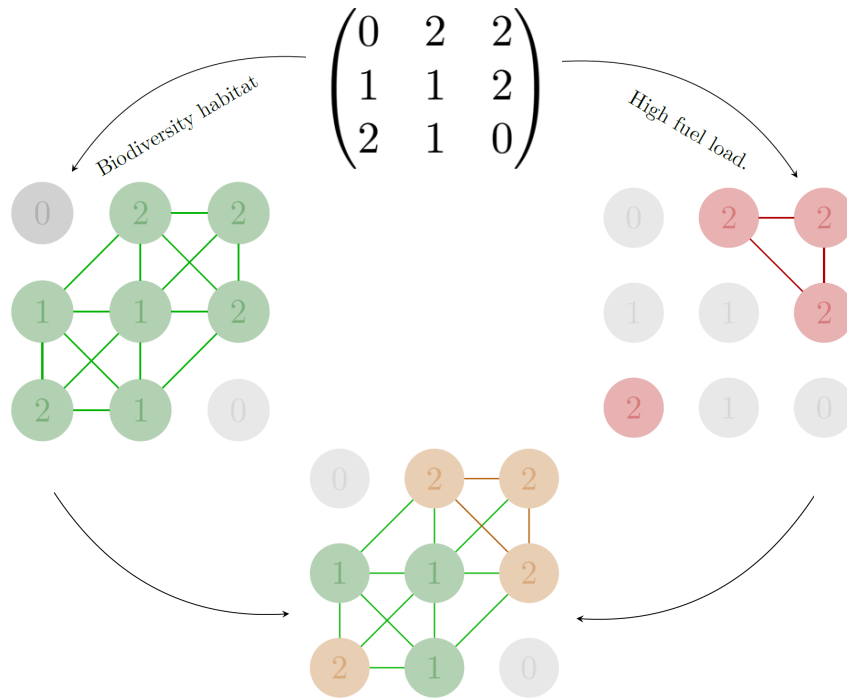
598 Denys Yemshanov, Ning Liu, Daniel K. Thompson, Marc-André Parisien, Quinn E. Barber, Frank H. Koch, and Jonathan Reimer.  
599 Detecting critical nodes in forest landscape networks to reduce wildfire spread. *PLOS ONE*, 16(10):e0258060, October 2021. ISSN  
600 1932-6203. doi: 10.1371/journal.pone.0258060. URL [https://journals.plos.org/plosone/article?id=10.1371/journal.pone.](https://journals.plos.org/plosone/article?id=10.1371/journal.pone.0258060)  
601 [0258060](https://journals.plos.org/plosone/article?id=10.1371/journal.pone.0258060). Publisher: Public Library of Science.

602 Denys Yemshanov, Robert G. Haight, Ning Liu, Rob Rempel, Frank H. Koch, and Art Rodgers. Exploring the tradeoffs among forest  
603 planning, roads and wildlife corridors: a new approach. *Optimization Letters*, 16(3):747–788, April 2022. ISSN 1862-4472, 1862-4480.  
604 doi: 10.1007/s11590-021-01745-w. URL <https://link.springer.com/10.1007/s11590-021-01745-w>.

605 Bo Zheng, Philippe Ciais, Frederic Chevallier, Hui Yang, Josep G. Canadell, Yang Chen, Ivar R. van der Velde, Ilse Aben, Emilio  
606 Chuvieco, Steven J. Davis, Merritt Deeter, Chaopeng Hong, Yawen Kong, Haiyan Li, Hui Li, Xin Lin, Kebin He, and Qiang Zhang.  
607 Record-high CO2 emissions from boreal fires in 2021. *Science*, 379(6635):912–917, March 2023. doi: 10.1126/science.ade0805. URL  
608 <https://www.science.org/doi/10.1126/science.ade0805>. Publisher: American Association for the Advancement of Science.

609 Yangming Zhou and Jin-Kao Hao. A fast heuristic algorithm for the critical node problem. In *Proceedings of the Genetic and Evolu-*  
610 *tionary Computation Conference Companion*, GECCO '17, page 121–122, New York, NY, USA, 2017. Association for Computing  
611 Machinery. ISBN 9781450349390. doi: 10.1145/3067695.3075993. URL <https://doi.org/10.1145/3067695.3075993>.

Figure 1: Illustration of the habitat and fuel graphs for  $n = 3$



In this graph, green cells support biodiversity habitat only, while red cells display high risk.

The high risk graph has two components (top right corner with 3 nodes, and bottom left corner with 1 node), while the biodiversity habitat graph only has one.

Cells for which the value is 0 are not considered as nodes for both graphs, and are thus not connected to the rest of the graphs. In the end, because high fuel load cells also support biodiversity habitat, the landscape can be represented as the overlap between the two graphs, where orange cells are high fuel load and also support biodiversity habitat.

Figure 2: Number of cycles as a function of biodiversity habitat and budget

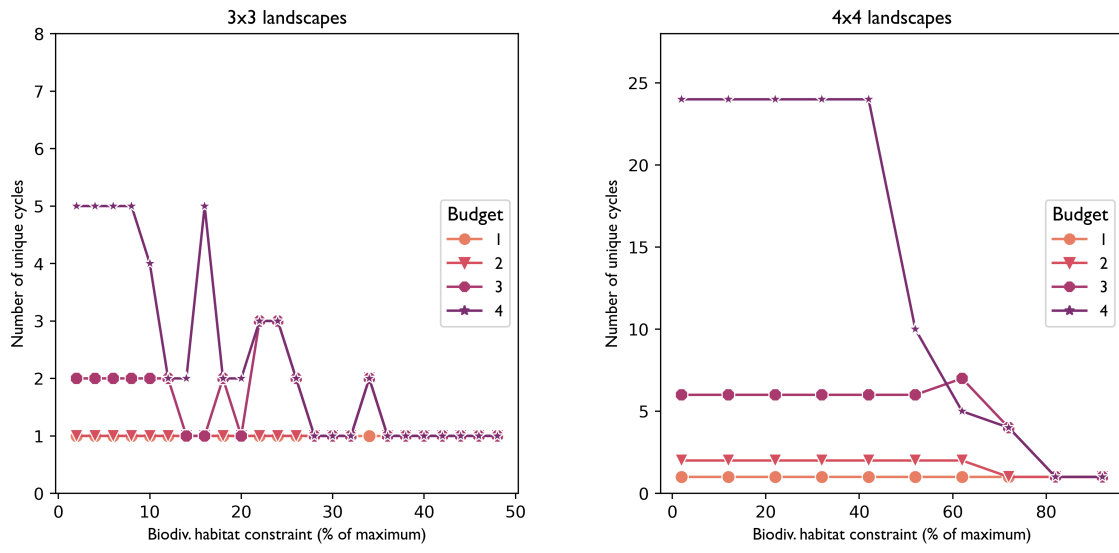


Figure 3: Production possibility frontier between constraint (as a % of maximum biodiversity sustainable in landscape) and wildfire risk for various budgets, and landscape size

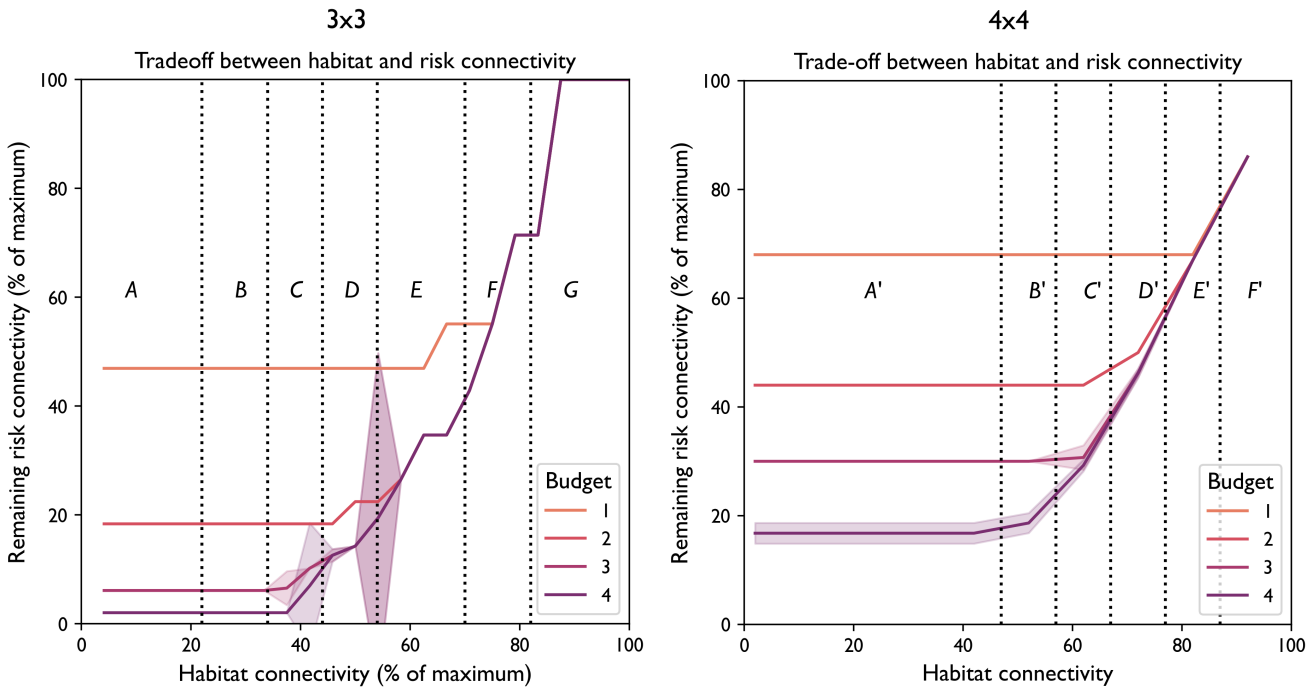


Figure 4: Most represented cycles for each biodiversity constraint level, for various budget and landscapes  $3 \times 3$ , and  $4 \times 4$  (95% CI shaded)

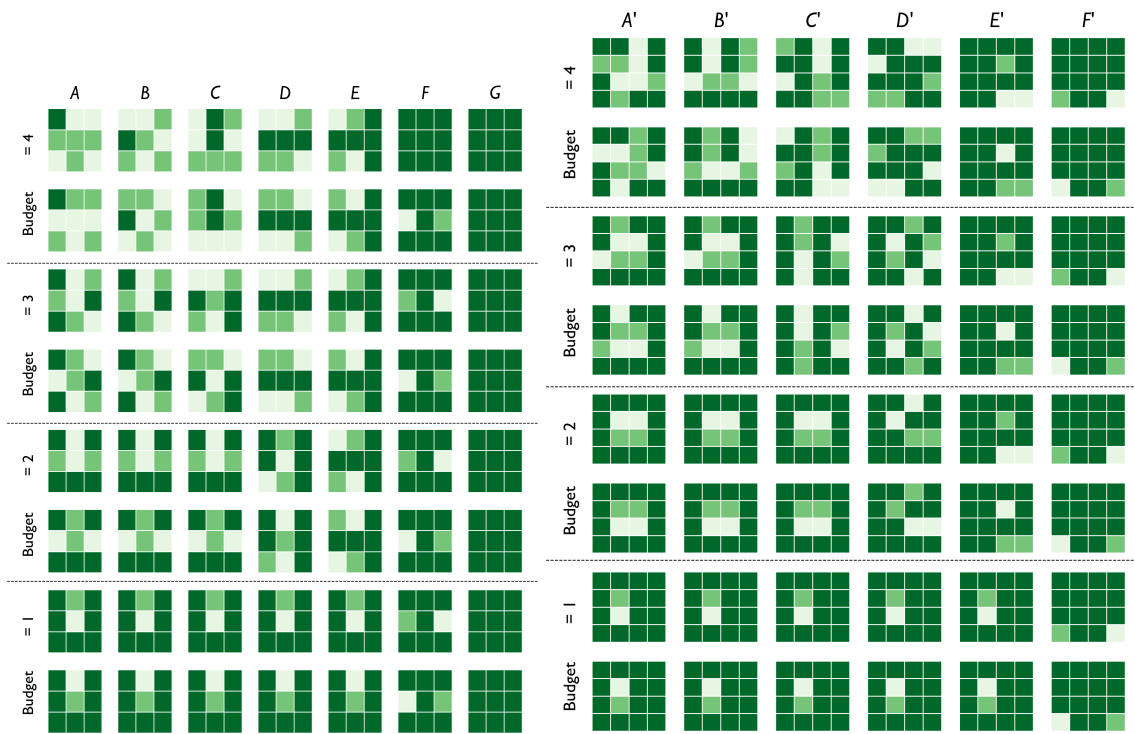


Figure 5: Assessment: surface, components of high-risk graph (95% CI shaded)

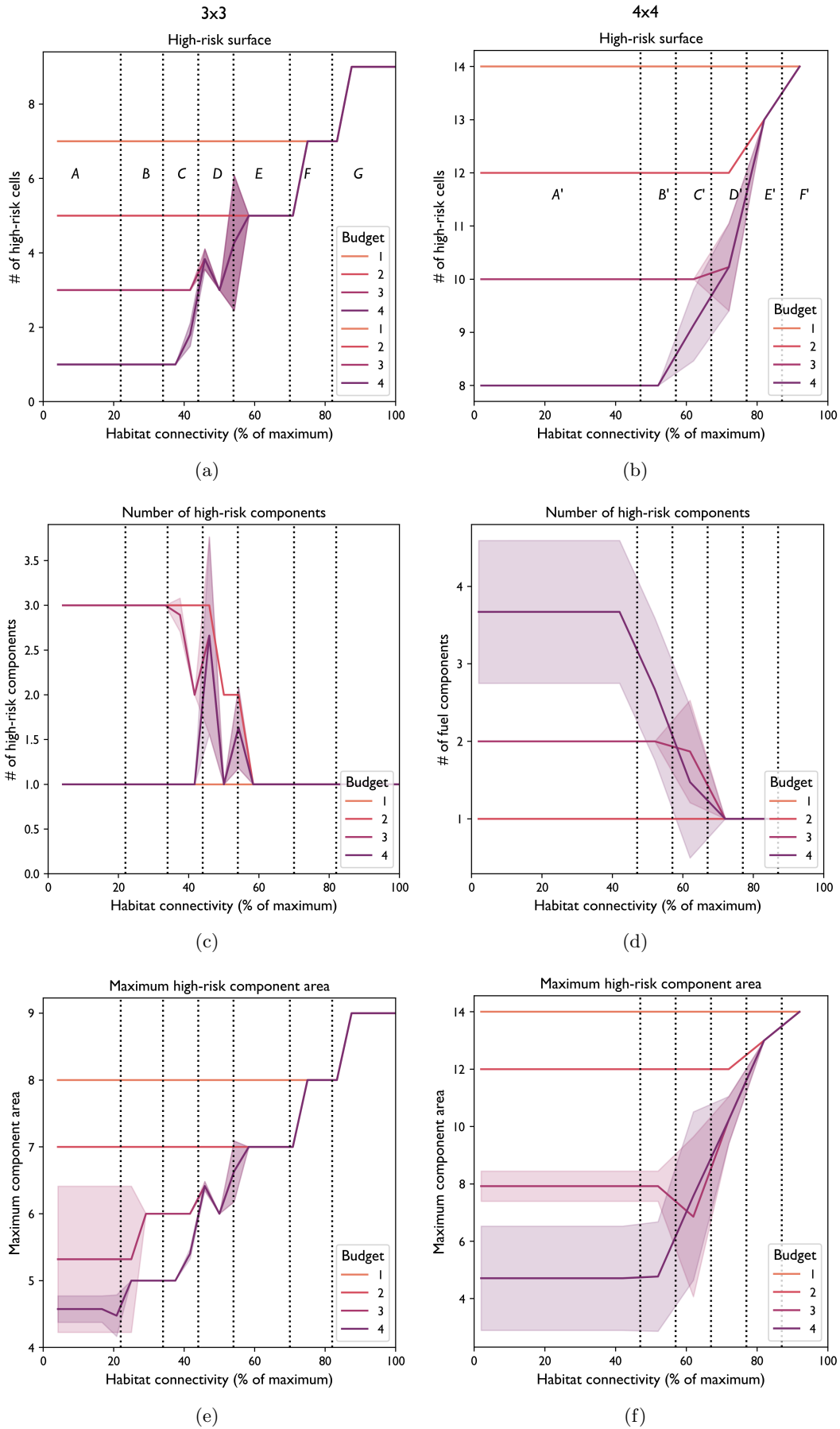


Figure 6: Assessment: diversity (95% CI shaded)

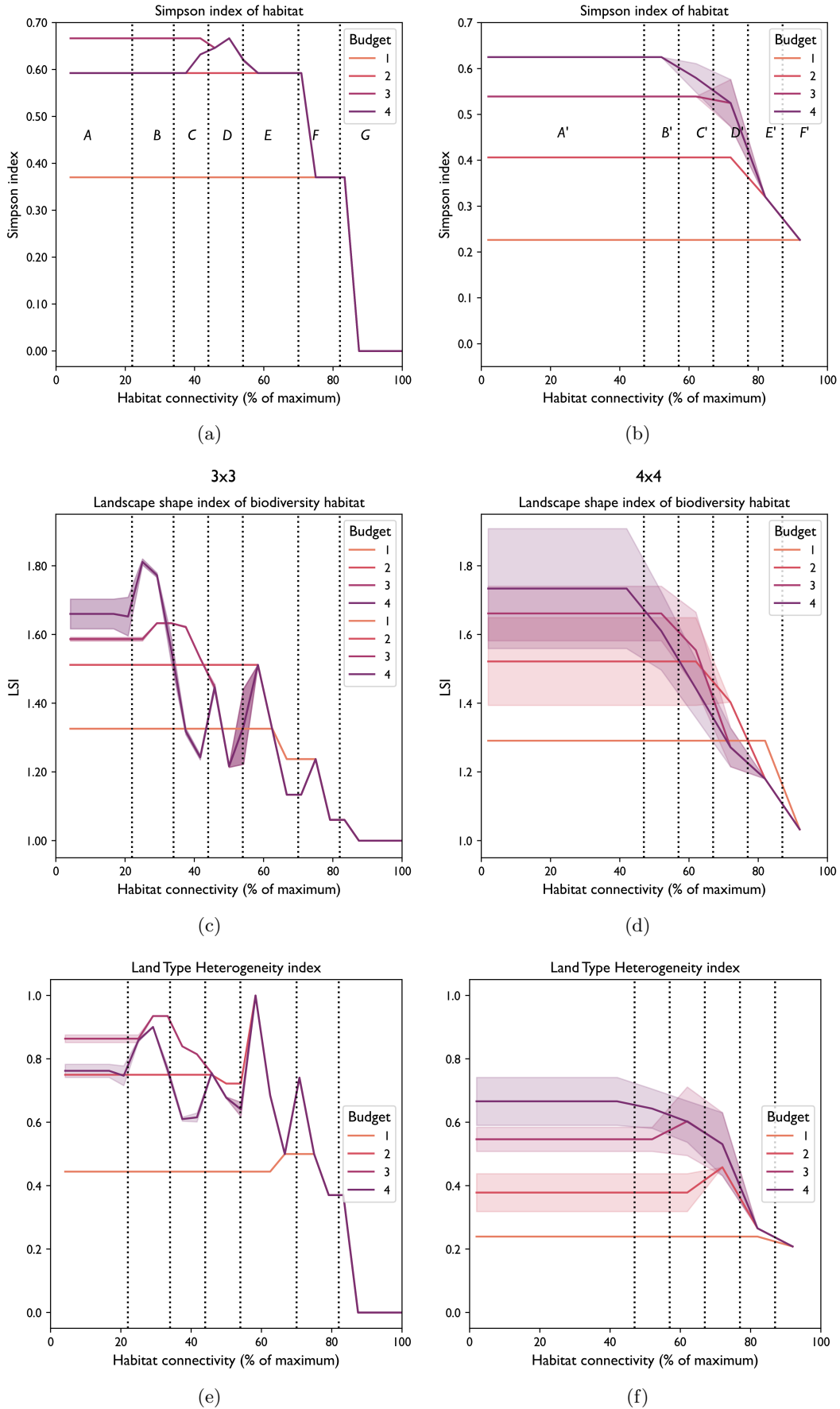


Figure 7: Treatment allocation : number, location

